Indian Journal of Experimental Biology
Vol. 63, June 2025, pp. 491-502
DOI: 10.56042/ijeb.v63i06.14845

Synthesis and biological evaluation of novel anthraquinone derivatives as potential therapeutics against breast cancer: *In vitro* and *in silico* approaches

Ebru Hacıosmanoğlu Aldoğan[1], Kamala Asgarova[2], Fidan Vagifli[2], Funda Özkök[2], Mesut Şentürk[3], Hilal Çap[4], Nihal Onul[2] & Başak Günçer[5]*

[1]Department of Biophysics, Cerrahpasa Faculty of Medicine, Istanbul University-Cerrahpasa, 34098, Istanbul, Türkiye

[2]Department of Chemistry, Faculty of Engineering, Istanbul University-Cerrahpasa, 34320, Istanbul, Türkiye

[3]Department of Pharmaceutical Chemistry, Faculty of Pharmacy, Istanbul Biruni University Istanbul, Türkiye

[4]Institute of Graduate Studies in Health Sciences, Istanbul University, Istanbul, Türkiye

[5]Department of Biophysics, Istanbul Faculty of Medicine, Istanbul University, Istanbul, 34093, Türkiye

Received 04 November 2024; revised 08 April 2025

Many traditional chemotherapeutic agents used for breast cancer cause systemic toxicity. Studies conducted on new-generation drug candidates have gained importance in recent years because of their low cytotoxicity and high anticancer effects. Anthraquinones and their derivatives are widely used for cancer treatment. In this study, we synthesized amino (5,7) and thioanthraquinone (3) derivatives. The effect of the compounds on cell viability was tested by the MTT assay using MCF-7 and MCF-10A cell lines. Compound 7 showed the highest inhibitory effect on cell proliferation MCF-7 with an IC_{50} value of 1.781 ± 1.4 and was therefore selected for further studies. The apoptotic effect of compound 7 was investigated using AnnexinV/Propidium Iodide (AV/PI) staining by flow cytometry, which revealed a significant increase in late apoptotic cells after 24h of treatment. Additionally, Caspase 3/7 activation was analyzed using fluorescence, which confirmed the induction of apoptosis by compound 7. In *silico* predictions of absorption, distribution, metabolism, and excretion (ADME) analysis confirmed the drug-likeness of compound 7. Molecular docking studies were conducted to understand interactions with target proteins. Compound 7 showed lower binding energy scores for Caspase 3, P53, Cytochrome C and Bax than the reference drugs These findings suggest that compound 7 holds promise as a potential therapeutic agent for breast cancer treatment. Further studies are warranted to elucidate its mechanism of action and explore its potential in clinical applications.

Keywords: Breast cancer, Anthraquinone derivates, Apoptosis, Molecular docking, ADME analysis

Breast cancer (BC) is the most common cancer in women worldwide. BC is divided into four types according to the expression of hormone receptors: human epidermal growth factor receptor 2 (HER2)-positive estrogen receptor 2-(ER)-positive, progesterone receptor (PR)-positive, and triple-negative breast cancer (TNBC; in which the receptors are not expressed). Regarding ER- and/or PR-positive BC, anticancer drugs targeting hormone receptors, such as tamoxifen, megestrol acetate, and raloxifene, have been developed[1]. Current cancer treatments include surgery, radiotherapy, and chemotherapy. Chemotherapy is the main approach for the treatment of metastatic BC; however, significant side effects such as neurotoxicity, bone marrow depression, and liver and kidney damage occur during the treatment process[2]. To eliminate these side effects, studies in medicinal chemistry have focused on the discovery of novel anticancer photochemicals that can specifically target cancer cells and minimize the possible side effects on normal cells[3]. Phytochemicals demonstrate anticancer properties through the regulation of disrupted signaling pathways that play key roles in cellular functions, including cell proliferation, cell cycle control, metabolic activity, and apoptosis (berberine).

Anthraquinones (AQs), such as valrubicin, doxorubicin, idarubicin, epirubicin, and mitoxantrone, have been successfully used to treat hematological and solid cancers. *Damnacanthal* is an example of a natural anthraquinone isolated from *Damnacanthus* that exhibits strong cytotoxic and apoptotic activities against breast cancer cell lines via activation of the *p53* and *p21* genes. These findings highlight the

*Correspondence:
Phone: +90 5323180546
E-mail: basak.varol@istanbul.edu.tr

potential of natural anthraquinones, such as emodin, aloe-emodin, and rhein, in inhibiting cancer cell growth and metastasis through various mechanisms. Emodin and aloe-emodin have been shown to inhibit breast cancer cell invasion and migration[4]. However, some pharmacological, pharmacokinetic, and toxicity studies, both *in vitro* and *in vivo* have shown that emodin may also have adverse effects on the reproductive system, kidney, and liver, especially when used over an extended period[5]. Aloe-emodin has shown promise in overcoming drug resistance in glioblastoma cells and has exhibited potent anticancer effects in pancreatic adenocarcinoma cell lines[6,7]. Rhein, on the other hand, has demonstrated efficacy against lung cancer cells by inhibiting the STAT3 pathway and inducing cell cycle arrest, as well as inducing oral cancer cell apoptosis and ROS generation via the AKT/mTOR signaling pathway in oral cancer[8,9]. The mechanism of apoptosis is complex and involves several pathways. This leads to the malignant transformation of the affected cells, tumor metastasis, and resistance to anticancer drugs. Moreover, it has been discovered that anthraquinones can also demonstrate anticancer efficacy via alternative pathways, such as paroptosis[10], autophagy, multidrug resistance[11], amplification of radiosensitivity[12] and suppression of invasion and metastasis[13] Collectively, these studies suggest several potential applications of these natural compounds in cancer treatment. Doxorubicin, epirubicin, and mitoxantrone are FDA-approved anthraquinone-derived drugs used in chemotherapy[14]. However, owing to the high preparation time, cost, and limited amount of natural compounds, synthetic chemicals have been used in drug discovery studies[15].

Functional groups such as amino, hydroxy, methoxy, cyano, thiazoline, and thiophene have been incorporated into the anthraquinone framework, significantly enhancing interactions with biological systems. Studies demonstrate that these specific anthraquinone derivatives exhibit improved biocompatibility along with selective antimicrobial and anticancer activity, highlighting their potential as promising candidates for biomedical applications[16].

In this study, three unique anthraquinone derivatives were synthesized, with the addition of thiol (compound 3) and piperazine amino groups (compounds 5 and 7) to enhance the biological activity. Previous studies have demonstrated the anticancer effects of both thiol and amino groups[17,18].

Materials and Methods

Synthesis method for the thioanthraquinone analog (3)

In a previous study, a practical, one-step, and economical synthesis method was developed to synthesize amino and thio-anthraquinone derivatives[19]. 1-Chloro anthraquinone compound 1, one molar equivalent of nonanethiol 2 and 25 mL ethylene glycol were stirred in a reaction flask. The reaction mixture turned yellow. Subsequently, 10 mL of aqueous potassium hydroxide solution was added to this yellow mixture and the reaction temperature was increased to 110–120°C. After reflux (48 h), an orange solid thioanthraquinone compound 3 was obtained (Fig. 1). The new product (3) was extracted using chloroform (30 mL). The organic layer was washed with water and dried with calcium sulfate. The novel synthesized analog (3) was purified by column chromatography.

1-(nonylthio)antracene-9,10-dione (3)

Orange solid. Yield: 0.9 g (62%), m.p: 114.1-114.6 ℃. R_f:0.48 (Chloroform); FT-IR (ATR):υ (cm^{-1}) =3077 ($CH_{arom.}$), 2956, 2921, 2850 ($CH_{aliphatic.}$), 1663 (C=O), 1590, 1570 (C=C); ^{1}H NMR (500 MHz, $CDCl_3$): δ=7.67-8.34 (m, 7H, $H_{arom.}$), 2.98-3.01 (m, 2H, S-CH_2), 1.27-1.82 (m, 14H, $CH_{nonanethiol}$), 0.87-0.88 (m, 3H, CH_3); ^{13}C NMR (125 MHz, $CDCl_3$): δ=183.52, 183.23, (C=O), 145.80 (S-$C_{arom.}$), 134.35, 133.62, 132.92 ($C_{arom.}$), 129.97, 127.44, 126.79 ($CH_{arom.}$), 32.16, 31.86, 29.45, 29.32, 29.29, 29.27, 27.82, 22.67 (CH_2), 14.12 (CH_3); ESI(+): *m/z*=384.5 $[M+NH_4]^+$, 239.95 $[M-(CH_2)_8-CH_3]^+$, $C_{23}H_{26}O_2S$, (M= 366.52 g/mol).

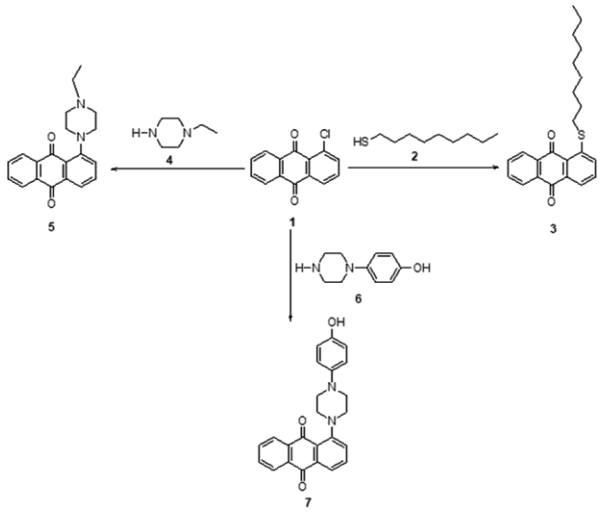

Fig. 1 — Synthetic pathway of anthraquinone analog.

Synthesis method for aminoanthraquinone analogs (5,7)

1-Chloro anthraquinone compound 1, one molar equivalent of 1-Ethylpiperazine (4) or 4-(piperazine-1-yl) phenol (6) and 25 mL ethylene glycol were stirred in the reaction flask. The reaction mixture turned yellow in colour. Subsequently, 10 mL of aqueous potassium hydroxide solution was added to this yellow mixture and the reaction temperature was increased to 110–120°C. After reflux (48 h), a violent viscous liquid compound 5 or a dark red solid compound 7 was synthesized. The novel products (5,7) were extracted with chloroform (30 mL). The organic layer was washed with water and dried with calcium sulfate, and the novel synthesized analogs (5,7) were purified by column chromatography.

1-(4-ethylpiperazin-1-yl)antracene-9,10-dione (5)

Viole viscos liquid. Yield: 0.73 g (57%), R_f :0.32 (Chloroform), FT-IR (ATR):υ (cm^{-1})=3069 ($CH_{arom.}$), 2922, 2851 ($CH_{aliphatic}$). , 1663, 1617 (C=O), 1590, 1570 (C=C); ^{1}H NMR (500 MHz, $CDCl_3$): δ=6.64-8.27 (m, 7H, $H_{arom.}$), 3.46-3.68 (m, 8H, $CH_{piperazin}$), 1.53-1.56 (m, 2H, CH_2), 1.23-1.26 (m, 3H, CH_3); ^{13}C NMR (125 MHz, $CDCl_3$): δ=185.24, 181.66 (C=O), 132.76, 125.72, 120.87, 110.76 ($C_{arom.}$ ve $CH_{arom.}$), 46.17, 45.20 ($C_{piperazin}$), 39.31 (CH_2), 10.38 (CH_3); ESI(+): *m/z*=321.30 $[M+H]^+$, 293.0 $[M-CH_2CH_3]^+$, 208.6 [M-ethylpiperazine]$^+$, $C_{20}H_{20}N_2O_2$, (M= 320.38 g/mol).

1-(4-(4-Hydroxyphenyl) piperazine-1-yl)antracene-9,10-dione (7)

Dark red solid. Yield: 1g (52%). m.p: 260-261°C. R_f: 0.46 (Dichloromethane). FT-IR(ATR): γ (cm^{-1})= 3412 (OH), 3280, 3279 (CH_{arom}), 1511, 1456 (C=C), 1603,1583 (C=O), 2996, 2955, 2929 ($CH_{aliphatic}$); ^{1}H NMR(499.74 MHz, $CDCl_3$)= s, 1H, OH), 7,45-7,48 (m, 4H, CH_{arom}), 4.03-4.30 (m, 8H, CH_2), 7.64-8.30 (m, 7H, CH_{arom}). ^{13}C NMR (125.66 MHz, $CDCl_3$) = 134.9, 134.1, 133.3, 129.4, 126.9, 122.8, 112.2 (C_{arom} and CH_{arom}),184.9, 182.7 (C=O), 150.8 (HO-C), 65.1 (CH_2). ESI (+): m/z= 385.10 $[M+H]^+$, $C_{24}H_{20}N_2O_3$), (M=384.15 g/mol).

Cell culture

The non-malignant breast epithelial cell line MCF-10A cells (CRL-10317, ATCC®, Manassas, VA, USA) was cultured in DMEM-F12 medium supplemented with 20 ng/mL epidermal growth factor, 0.5 µg/mL hydrocortisone, 10 µg/mL insulin, penicillin/streptomycin (100 U/mL and 100 mg/mL), and 1 % L-glutamine all purchased from Sigma, St. Louis, MO, USA). Human breast adenocarcinoma cells, MCF-7 (HTB-22, ATCC®, Manassas, VA, USA) cells were cultured in DMEM F-12 (Thermo Fisher Scientific, Waltham, MA, USA) medium supplemented with fetal bovine serum (10%, FBS, Sigma, St. Louis, MO, USA) and penicillin/streptomycin (100 U/mL and 100 mg/mL, Sigma, St. Louis, MO, USA) at 37°C with 5 % CO_2 in standard cell culture conditions[20].

Cell viability assay

A colourimetric assay, 3-(4,5-Dimethylthiazol-2-yl)-2,5-Diphenyltetrazolium Bromide (MTT; Sigma, St. Louis, MO, USA), was performed[21]. MCF-7 cells were seeded in 96-well plates at a density of 3×10^5 cells/well and incubated with certain concentrations of compounds 3, 5 and 7 individually (1-50 µM) for 24 h. After treatment, MTT (final concentration 0.1 mg/mL) was added, and the cells were incubated for 4 h at 37°C. Following aspiration of the supernatants, DMSO was added, and the mixture was further incubated at room temperature in the dark for 30 min. Absorbance was measured at 570 nm using a microplate reader (BioTek Instruments Inc., VT, USA), and IC_{50} values were calculated using Excel and GraphPad Prism 7 (GraphPad Software, La Jolla, CA, USA). The significance of the differences between the control and treatment groups was analyzed by one-way ANOVA with GraphPad Prism 7, and a *P* value less than 0.05 was considered significant.

Apoptosis detection (Annexin V-FITC/PI staining)

The apoptosis assay was performed using a fluorescein isothiocyanate (FITC) Annexin V Apoptosis Detection Kit (ApoFlowEx FITC Kit, ExBio, Czech Republic). Briefly, 5×10^5 cells were washed with cold PBS and suspended in 100 µL Annexin V binding buffer. The cells were stained with 5 µL FITC-labeled Annexin V and 5 µL propidium iodide (PI) and incubated for 15 min at room temperature in the dark. PI was used with Annexin V to determine whether cells were viable, early apoptotic, late apoptotic, or necrotic. The cells were analyzed using a flow cytometer (BD Accuri C6 Plus Flow Cytometer, CA, USA). In this assay, Annexin V and PI negative (V^- P^-) cells are considered viable cells, and Annexin V positive and PI negative (V^+ PI^-) cells are considered to be in the early stages of apoptosis. Annexin V and PI positivity (V^+ P^+) are considered in the late apoptosis or death stage[22]. NovoExpress software was used to analyze the results.

Caspase-3/7 activation assay

The percentage of caspase-3/7 activation was determined using a Caspase-3/7 kit (Promega, Madison, WI, USA) according to the manufacturer's instructions. Caspase-3/7 activation detects a luminogenic substrate that is cleaved by caspases, resulting in the generation of a luminescent signal. The signal was measured using a fluorescence microplate reader (BioTek Instruments, Inc., VT, USA) at 490 nm.

Drug-like properties

To elucidate the structure-activity relationships of compound AA, drug-likeness evaluations were performed using the Swiss ADME Calculation program[23] (http://www.swissadme.ch).

Molecular docking studies

Molecular docking simulations, energy minimization, and molecular visualization were conducted using AutoDock Vina software suite[24]. Compound 7 was prepared for molecular docking using the ChemDraw sketch program, while the Chem3D suite was used to draw and edit the compound in SD file format. These molecular structures underwent protonation, charging, and conformation minimization based on the root-mean-square gradient. The three-dimensional coordinates of the X-ray crystal structures of the target proteins were obtained from the Protein Data Bank (RCSB) (https://www.rcsb.org). The crystal structures used in the docking calculations included CDK2 (PDB:1AQ1), PI3K (PDB:1EZ8), Caspase 3 (PDB: 1 NMS), Cytochrome C (PDB:1OCD), P53 (PDB: 1T4E), topoisomerase 2 (PDB: 1ZXM), and Bax (PDB:3G11). Structural defects in these target proteins were rectified using the AutoDock Vina software. Docking calculations were performed using default parameters (temperature, 300 K; *p*H: 7.0, solvent: 0.1 M, electrostatic energy cutoff, 15 Å). The final molecular docking scores were derived as the average of the top 10 docking poses based on the binding minimum energy (kcal/mol) for each compound. Conformations with the lowest negative binding energy values, indicative of the strongest binding affinity of the ligand to the target, were selected following the docking interactions.

Results

Synthesis and characterization

In this study, three anthraquinone derivatives were synthesized. In the FT-IR (ATR) spectrum of compound 3, the stretching bands of the υ=2956, 2921, and 2850 aliphatic ($CH_{aliphatic}$.) bonds were observed. In the ^{1}H NMR ($CDCl_3$) spectrum of 3, the (CH_3) protons in the aliphatic chain of nonantiol were confirmed as multiplets at δ=0.87-0.88 ppm and the (CH_2) protons close to sulfur were confirmed as multiplets at δ=2.98-3.01 ppm. Other methylene protons in the non-ano chain were observed at δ=1.28-1.57 ppm. In the ^{13}C NMR ($CDCl_3$) spectrum of compound 3, a sulfur-bound carbon in the anthraquinone ring was observed at δ=145.80 ppm. The (CH_3) carbon in non-ano was observed at δ=14.12 ppm. The ESI(+) polarity mass spectrum of 3 ($C_{23}H_{26}O_2S$, M=366.52 g/mol) showed an *m/z*=384.15 $[M+NH_4]^+$ molecular ion and an m/z=239.95 $[M-(CH_2)_8CH_3]^+$ fragmentation ion. In the FTIR (ATR) spectrum of 5, stretching bands of aliphatic ($CH_{aliphatic}$.) bonds were observed at υ=2922, 2851 cm^{-1}. In the ^{1}H NMR ($CDCl_3$) spectrum of compound 5, the methylene protons in the piperazine ring were confirmed as a multiplet at δ=3.46-3.68 ppm and CH_3 protons in the ethyl chain attached to the piperazine ring were confirmed as a multiplet at δ=1.23-1.26 ppm and CH_2 methylene protons were confirmed as a multiplet at δ=1.53-1.56 ppm. In the ^{13}C NMR ($CDCl_3$) spectrum of compound 5, the methylene carbon of the chain attached to the piperazine ring was observed at δ=39.31 ppm and the methyl carbon was observed at δ=10.38 ppm. The carbons in the piperazine ring were observed at δ=46.17, 45.20 ppm. The ESI (+) polarity mass spectrum of compound 5 ($C_{20}H_{20}N_2O_2$, M=320.38 g/mol) showed an m/z=321.15 $[M+H]^+$ molecular ion and m/z=293.0 $[M-CH_3CH_2]^+$ and *m/z*=208.6 $[M-C_4H_9N_2CH_2CH_3]^+$ fragmentation ions. In the FTIR (ATR) spectrum of 7, the stretching band of the (OH) bond was observed at υ= 3412 cm^{-1}. ^{1}H-NMR ($CDCl_3$) spectrum of 7 showed that the OH group in the piperazine ring was observed as a singlet at δ = 1.57 ppm. In the ^{13}C-NMR ($CDCl_3$) spectrum of compound 7, the carbonyl group carbons (C=O) in the anthraquinone ring were observed at δ=184.9,182.7 ppm and the nitrogen-bonded carbon (C-N) at δ=142.9 ppm. The aromatic carbons of anthraquinone and 4-hydroxophenylpiperazine are observed at δ=134.9, 134.1, 133.3, 129.4, 126.9, 122.8, and 112.2 ppm. In 4-hydroxophenylpiperazine, hydroxylated methylene was observed at δ=150.8 ppm and other carbons at δ=65.1 ppm. The mass spectrum of compound 7 ($C_{24}H_{20}N_2O_3$) (M=384.15 g/mol) at ESI(+) polarity showed *m/z*= 385.10 $[M+H]^+$ (Fig. 1).

Effects of compounds 3, 5 and 7 on the cell viability of non-tumorigenic breast epithelial and breast cancer cell lines

The effect of the compounds on cell proliferation was explored using the MTT assay. MCF-7 breast cancer cells and MCF-10 A healthy control cells were incubated with compounds 3, 5 and 7 individually at concentration of 3-150 µM for 24 h. The compounds exhibited concentration-dependent cytotoxic profiles in cell lines. When compound 3 was applied, cell viability decreased significantly with increasing concentrations ($^{***}P< 0.001$) in both cell lines. These data show that just as compound 3 decreased the cell viability of cancer cells, it also caused death in healthy cells.

In contrast, no significant changes were observed after treatment with compounds 5 and 7 separately in MCF-10A cells (Fig. 2A). Although compounds 5 and 7 showed concentration-dependent inhibitory effects on MCF-7 cell viability, compound 7 had better antiproliferative activity than compound 5 ($^{+++}P < 0.001$, Fig. 2B).

The half-maximal inhibitory concentration (IC_{50}) values obtained for all the tested compounds are listed in Table 1. Compounds 3, 5 and 7 exhibited cytotoxic activities with IC_{50} values of 2.7, 8.832, and 1.781 respectively against MCF-7 cells. Compound 7 showed the highest inhibitory effect on MCF-7 cells.

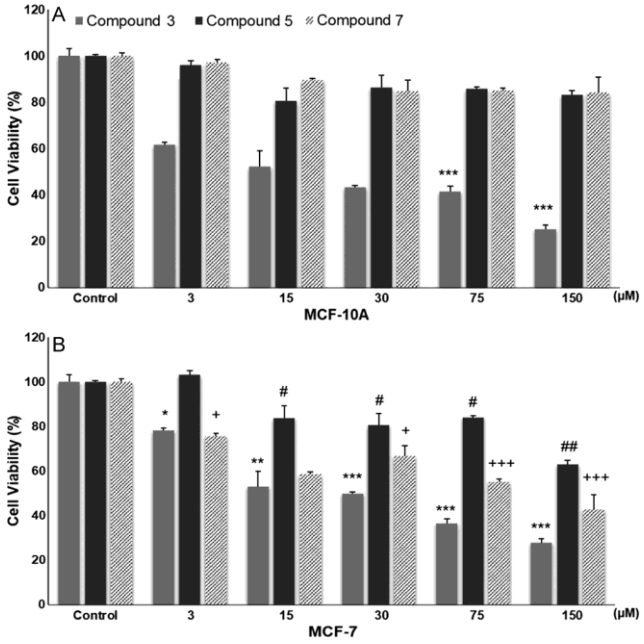

Fig. 2 — Cell viability of (A) MCF-10A (B)MCF-7 cells after treatment with compounds 3, 7, and 5 for 24 h. Significant differences in control of compounds 3,7 and 5 respectively, indicate *, $^{\#}$, $^{+}$ $P < 0.05$; **, $^{\#\#}$, $^{++}$ $P < 0.01$; ***, $^{\#\#\#}$, $^{+++}$ $P < 0.001$.

Moreover, it did not show any toxic effects on non-cancerous MCF-10A cells. Based on these results, we decided to conduct future studies using compound 7.

Induction of apoptosis by compound 7 in breast cancer cells

Apoptosis is a crucial process that regulates programmed cell death, and previous studies have revealed the anticancer effect of anthraquinones using flow cytometry. Owing to the strong inhibitory effect of compound 7 against MCF-7 cells, further studies were carried out to analyze the apoptotic rates with AV-PI dual staining by flow cytometry. 5×10^5 MCF-7 cells were treated with increasing concentrations of compound **7** (3-150 µM) for 24 h. As shown in (Fig. 3A-F) the number of apoptotic cells increased in a dose-dependent manner. The proportion of MCF-7 cells in early apoptosis was 8.6 %, in late apoptosis was 67.22 %, and necrosis was 7.92 % after 24 h incubation time respectively (Fig. 3G).

Effect of Compound 7 on caspase-3/7 activation

Caspases-3 and 7 are effector caspases are essential for the cleavage of cellular targets. The late phase begins with activation of caspase-3/7, resulting in DNA fragmentation[25]. The mechanism of apoptotic induction by compound 7 was investigated by determining the percentage of caspase-3/7 activation in cancerous cell lines treated with the IC_{50} dose of compound 7. results (Table 2) revealed that compound 7 significantly induced caspase-3/7 activation (more than 50%) higher than that reference; doxorubicin ($IC_{50} = 0.0266$ µM) (40.62 %) in breast cancer cell lines. Accordingly, the results of the caspase-3/7 activation assay were concordant with those of flow cytometric analysis of apoptosis.

Drug-Like Properties

ADME of Absorption, Distribution, Metabolism, and Excretion (ADME) of drug candidates is crucial for selecting appropriate candidates for preclinical studies. In this study, the ADME parameters of a new amino-anthraquinone derivative were assessed using the Swiss ADME Calculation program. The molecular weight, log *P*, Topological polar surface area (TPSA), blood-brain barrier (BBB) permeability,

Table 1 — Cytotoxic IC_{50} values of the compounds tested against MCF-7 and MCF-10A lines using the MTT assay

Compound	IC_{50} (µM)	
	MCF-10A	MCF-7
3	1.178 ± 0.12	2.7 ± 2.1
5	2.138 ± 0.34	8.832 ± 0.2
7	9.005 ± 0.92	1.781 ± 1.4

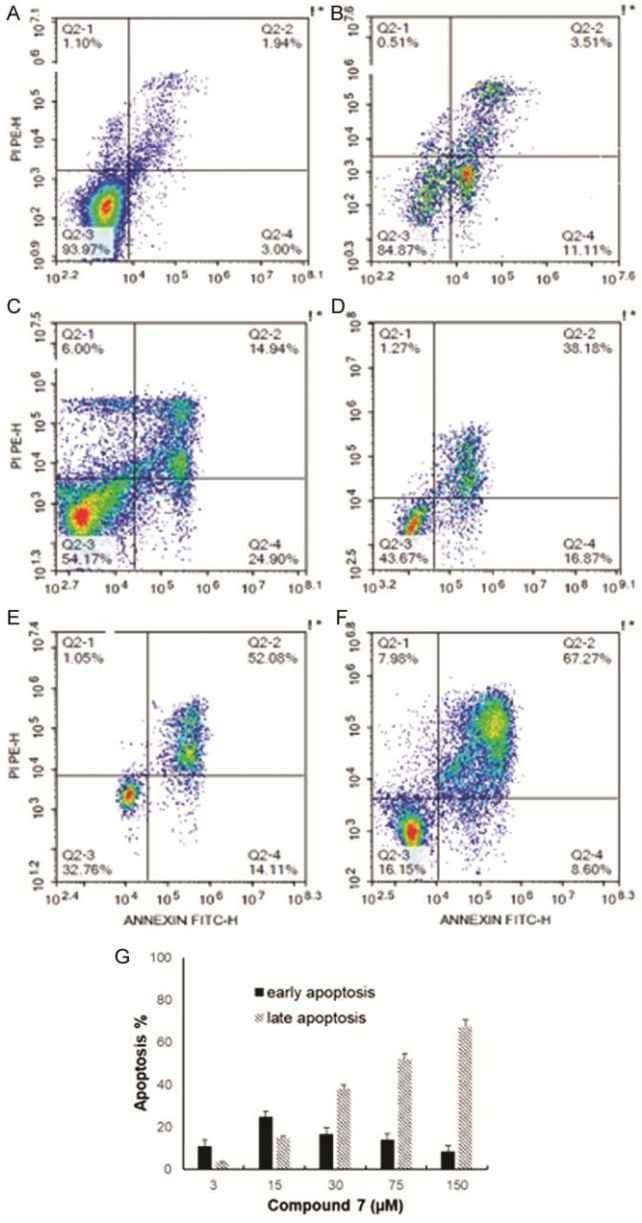

Fig. 3 — (A-F) Compound 7 induced apoptosis of MCF-7 cells evaluated by Annexin V-FITC/PI double staining assay. (G) Annexin V/PI staining representative dot plots: Q2-4 (early apoptosis), Q2-3 (live), Q2-2 (late apoptosis), and Q2-1 (necrosis). (A) Control, (B) 3 μM (C) 15 μM, (D) 30 μM, (E) 75 μM, (G) 150 μM compound 7 treated MCF-7 cells for 24 h. (G) Percentage column bar graph of early and late apoptotic cell death. Data are shown as mean ± SEM, $^{**}P < 0.01$ compared with the corresponding control.

gastrointestinal (GI) absorption properties, and CYP-450 enzyme inhibition profile of compound 7 are summarized in Table 3. According to the drug-likeness criteria, the molecular weight of a compound should range from 150 to 500 g/mol, and compound 7 should exhibit a molecular weight of 384.43 g/mol. The log*P*[b] value should be less than 5; for compound 7, it was calculated to be 3.12. The total polar surface area (TPSA) should be between 20 and 130 Å², with compound 7 displaying a TPSA of 60 Å². Compound 7 demonstrated the ability to cross the BBB and showed high GI absorption, indicating that it could effectively traverse lipid barriers. Furthermore, compound 7 inhibited CYP1A2, CYP2C9, and CYP3A4 expression. Importantly, compound 7 complied with Lipinski's Rule of Five.

Molecular Docking Studies

The anti-proliferative effects of this novel compound were explored using molecular docking studies, and the best-docked poses of the molecules were thoroughly evaluated. The binding affinity and receptor-ligand interactions of compound 7 were assessed, revealing strong interactions within the active sites of the target receptor proteins, as shown in Table 4.

Compound 7 had a lower energy score than the reference drugs for targets Caspase-3, cytochrome C, P53, and Bax, while having higher energy scores for the rest. The interaction of compound 7 with apoptotic targets was consistent with our previous apoptotic findings. As demonstrated in (Fig. 4-8) molecules bound to the active site overlapped with the reference molecules. Our initial findings indicate that these compounds have reasonable ligand-receptor binding interactions. The oral bioavailability radar chart was predicted with SwissADME, as shown in (Fig. 8) This graph uses six physicochemical characteristics of a

Table 2 — Percentages of caspase-3/7 activation in compound 7 treated MCF-7 cell line

	MCF-7 cells
Compound 7	58.98 ± 1.22
Doxorubicin	40.67 ± 0.74

[All values are expressed as mean ± SEM]

Table 3 — Drug-like properties of compound 7 calculated by the Swiss ADME online software program

Compound	MW[a] (g/mol)	LogP[b]	TPSA[c]	BBB[d]	GI Abs.[e]	Type of CYP Inh.[f]	Rule of Five[g]
Compound 7	384.43	3.12	60.85	Yes	High	CYP1A2, CYP2C9, CYP3A4	Yes

[[a]Molecular weight (recommended value <500); [b]Logarithm of the partition coefficient of the compound between n-octanol and water (recommended value <5); [c]Polar surface area (recommended value ≤140Å^2); [d]Indicates whether the compound passes Blod Brain Barrier or not; [e]Degree of Gastrointestinal Absorption; [f]Represent the inhibition of CYP450 subtypes; [g]Indicates whether the compound obeys Lipinski's Rule of Five or not]

Table 4 — Docking results for compound 7 and reference drugs against various target proteins

Target Protein And Ligand	Structures	Docked amino acid residues (vdW interactions)	Energy Score (kcal/mol)	RMD Value	H bond (distance Å)
CDK2 (PDB:1AQ1) Compound 7	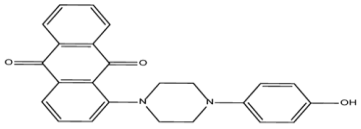	LYS33,PHE82, LEU83	-10.29	1.68	H of OH with O of Carboxyl of ASP145 (2.212)
CDK2 Palbociclib	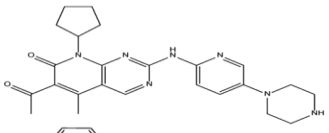	PHE80, PHE82, LEU83	-12.57	0.11	O of Carbonyl with H of NH of ASP145 (1.713)
PI3K (PDB:1EZ8) Compound 7	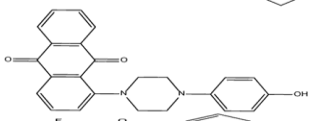	ASP841, TYR867, ILE963, ASP964	-10.68	0.96	None
PI3K İdealisib	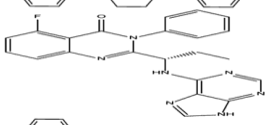	TYR867, MET953, ILE963	-11.29	0.30	O of Carbonyl with H of NH of VAL882 (1.923)
Caspase-3 Compound 7	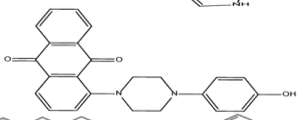	TYR204, TRP206, ARG207,	-10.09	0.34	O of Carbonyl with H of NH of HIS121 (2.149)
Caspase-3 Pac-1	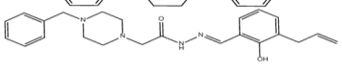	ARG64, HIS121, ARG207	-9.35	0.37	H of NH with O of Carbonyl of ASN208 (1.938)
Cytochrome C Compound 7	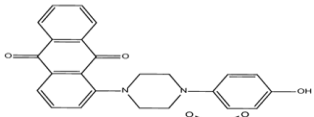	TYR67, THR78, LYS79	-12.73	0.07	None
Cytochrome Methazolamide	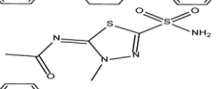	TYR67, LEU68, THR78	-10.34	0.82	None
P53 Compound 7	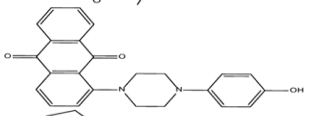	LEU54, GLY58, MET62	-9.79	0.08	H of OH with O of Carbonyl of GLY16 (2.153)
P53 Pifithrin	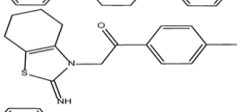	GLY16, LEu54, MET62	-7.86	0.67	None
Topoisomerase 2 Compound 7	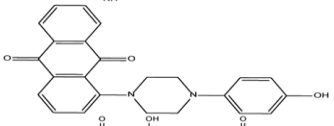	SER149, GLY164, TYR165,	-11.25	0.61	O of OH with H of NH of GLY166 (1.939)
Topoisomerase 2 Dox	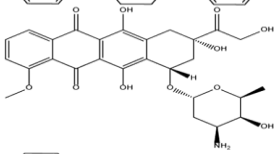	GLY161, TYR165, GLY166	-13.69	0.88	O of OH with H of NH of ALA167 (1.711)
Bax Compound 7	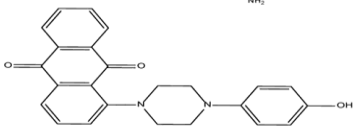	ALA207, PHE229, THR307	-10.65	0.12	O of Carbonyl with H of NH of HIS303 (1.671)
Bax B-7	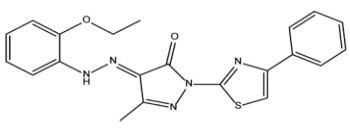	ALA207, HIS303, THR307	-9.85	0.48	None

[**Structures containing the CDK2 (PDB: 1AQ1), PI3K (PDB: 1EZ8), Caspase 3 (PDB: 1INMS), Cytochrome C (PDB: 1OCD), P53 (PDB:1T4E), Topoisomerase 2 (PDB: 1ZXM), Bax (PDB:3G11) were chosen as crystal structure models corresponding to this target protein for use in docking calculations]

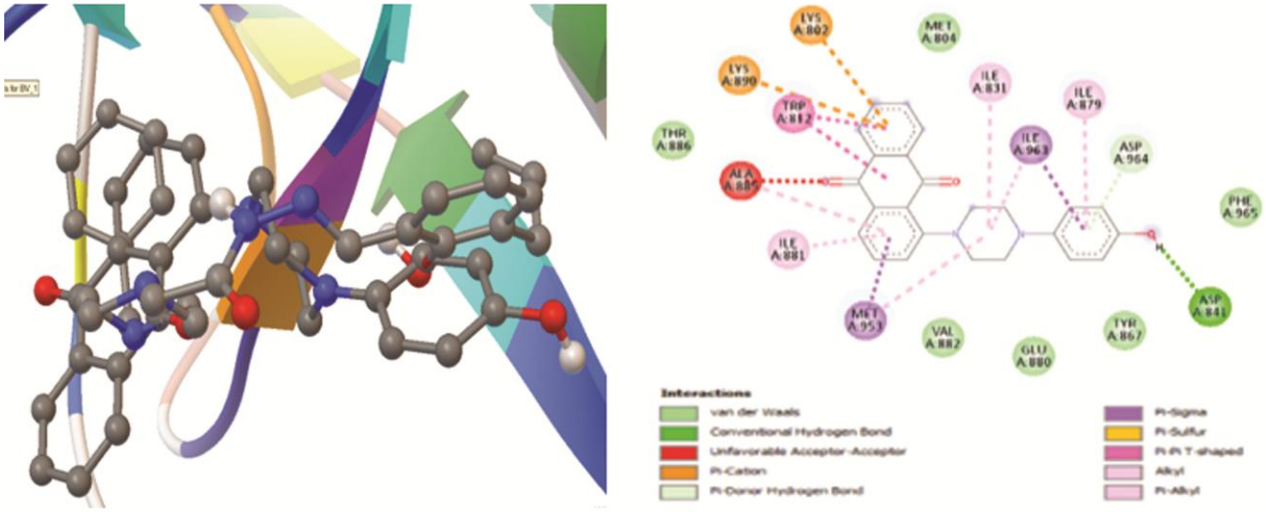

Fig. 4 — Compound 7 interaction with Caspase-3 (PDB 1INMS). (A) 3D Interaction (B) 2D interaction.

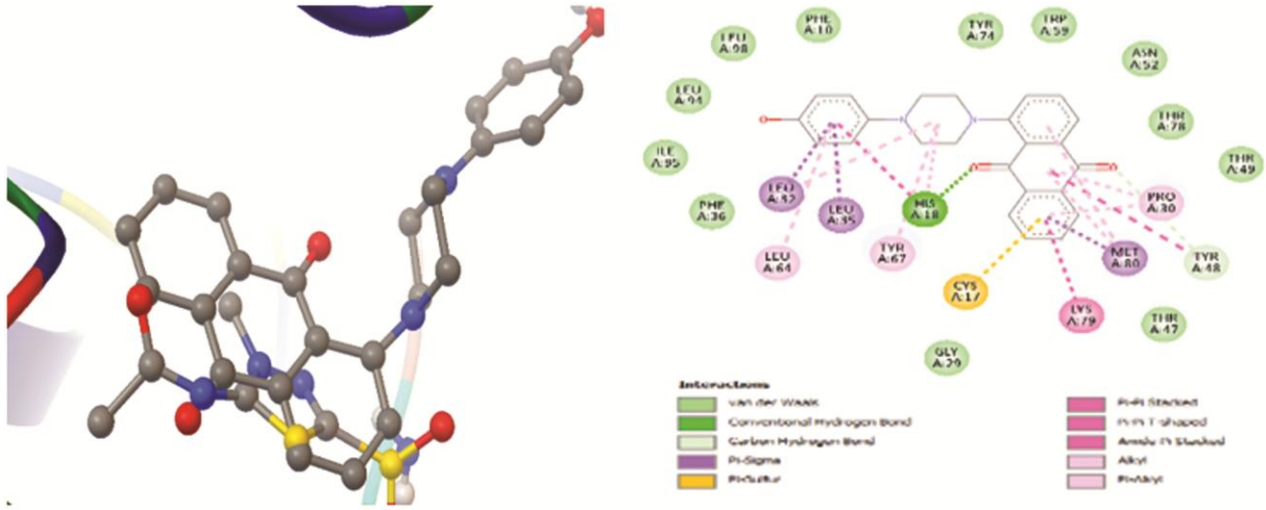

Fig. 5 — Compound 7 interaction with Cytochrome C (PDB 1OCD). (A) 3D Interaction (B) 2D interaction.

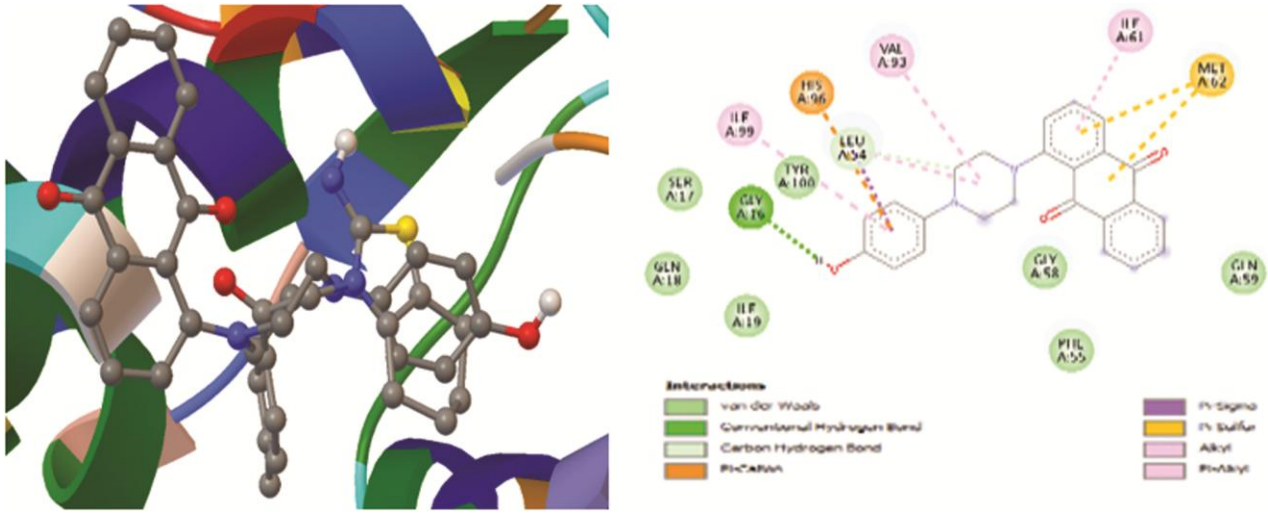

Fig. 6 — Compound 7 interaction with P53 (PDB1T4E). (A) 3D Interaction (B) 2D interaction.

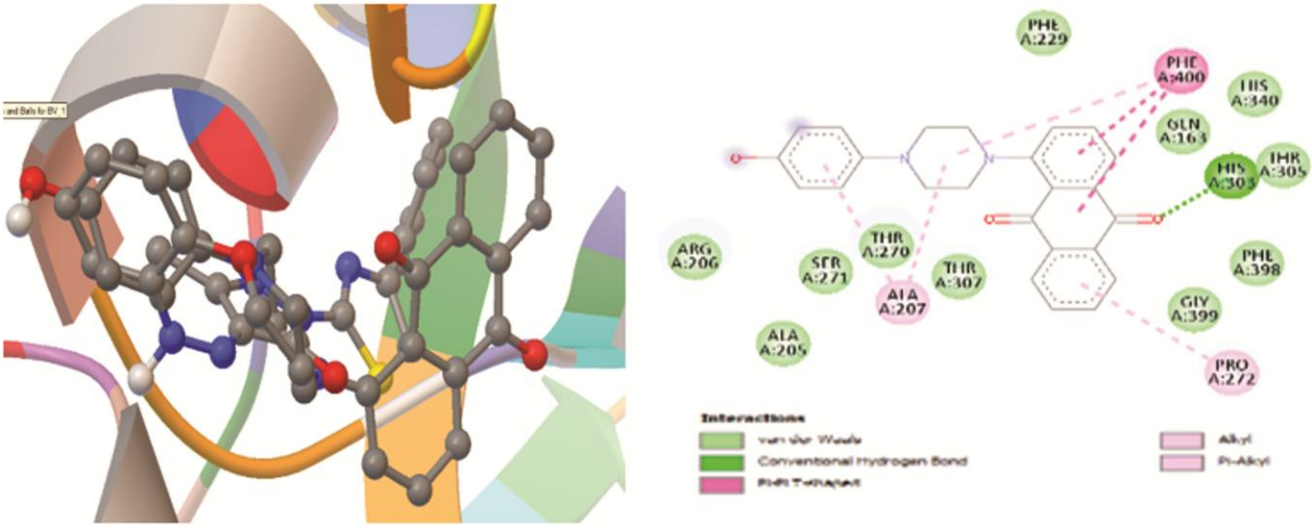

Fig. 7 — Compound 7 interaction with Bax (PDB 3G11). (A) 3D Interaction (B) 2D interaction.

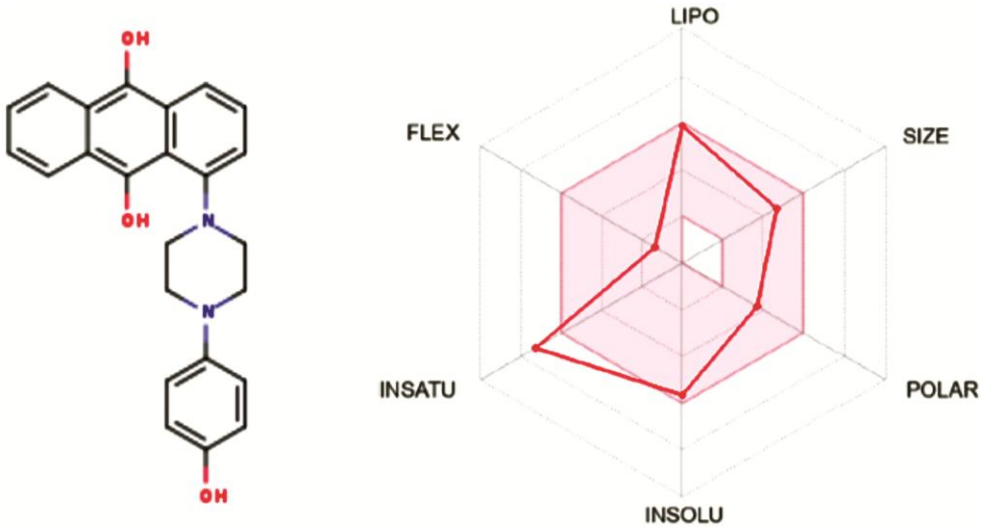

Fig. 8 — Oral bioavailability radar of compound 7 predicted using the Swiss ADME database. (A) Chemical structure of compound 7; (B) The pink zone is the favorable physicochemical space for oral drug bioavailability, and the red line represents the oral bioavailability properties of the derivatives. [FLEX; flexibility, LIPO; lipophilicity, INSATU; unsaturation, INSOLU; insolubility, POLAR; polarity]

molecule *i.e.*, flexibility, unsaturation, insolubility, lipophilicity, polarity, and size. The physicochemical properties of compound 7 were within the limit defined by the pink region, except that unsaturation was an outlier. The pink zone in the chart represents a suitable physicochemical space for the bioavailability of oral drugs.

Discussion

Anthraquinones are compounds that have been used as core chemical templates to achieve structural modifications, such as promising anticancer agents. The number of new anthraquinone-based compounds has been rapidly increasing in recent years. Several derivatives have been synthesized and investigated for their anticancer properties[26]. Doxorubicin 7 is an anticancer drug with an anthraquinone nucleus produced by bacteria of the Streptomyces genus. It binds to DNA-associated enzymes and intercalates with the DNA base pairs[27]. The antitumor activities of anthraquinones include a wide range of areas such as inhibition of cancer cell proliferation, induction of apoptosis, invasion, migration and reversing drug resistance. Moreover, anthraquinones directly inhibit various targets in the cell, such as

protein kinases, topoisomerases, matrix metalloproteinases (MMPs), and ectonucleotidases[28].

In this study, we synthesized new anthraquinone derivatives, namely compounds 3, 5, and 7. Anticancer potential of the derivatives was investigated. Compound 7 showed the highest antiproliferative activity and high selectivity index against MCF-7 cells and did not show a toxic effect against non-cancerous MCF-10A cells. Based on these results, we decided to conduct future studies using compound 7. Apoptosis is considered a major mechanism of chemotherapy-induced cell death. The apoptotic effect of compound 7 was investigated by AV/PI staining using flow cytometry and a caspase 3/7 activation assay for 24 h. It has been shown that compound 7 induced apoptosis in 24 h. Likewise, in our study, 1,3-dihydroxy-9,10-anthraquinone-2-carboxylic acid (DHAQC) (2), an anthraquinone derivative, showed apoptotic induction in MCF-7 cells[15]. Consistent with our results, in a recent study, induction by caspase-3 activation was defined as a good biomarker for early apoptosis that accurately predicted tumor growth inhibition by anti-cancer drugs in engineered colon cancer and glioblastoma cell lines and mouse xenograft models[29].

ADME analysis of drug candidates provides data for selecting appropriate candidates for preclinical studies. In a previous study, two series of novel anthraquinone-based benzenesulfonamide derivatives were designed, with ADME predictions indicating favorable pharmacokinetic and physicochemical properties for all compounds[30]. In this study, we identified the ADME parameters of a new amino-anthraquinone derivative. According to Lipinski's rule of five, the number of hydrogen-binding atoms should not exceed five. The molecular weight of the compound should be between 150 and 500 g/mol. Compound 7 had a molecular weight of 384.43 g/mol. The total polar surface area (TPSA) should be between 20 and 130 Å2, and it was found to be 60.85 A° for compound 7. GI absorption was high, and it was observed that compound 7 could pass through the blood-brain barrier. These results indicated that compound 7 has drug-like properties, consistent with previous studies, such as 9,10-anthraquinone, an endogenous estrogen receptor ligand[31]. *In silico* drug design tools have also made a great contribution to the development of new anthraquinone derivates[32].

Using molecular docking studies, it is possible to predict how a ligand binds to a three-dimensional protein using the molecular docking method. Target proteins were selected based on previous studies[24]. Caspase-3, the apoptosis regulator Bcl-2, cyclin-dependent protein kinase 2 (CDK2), cytochrome c, P53, topoisomerase 2, and Bax were chosen as molecular targets for compound 7**.**

According to our results, compound 7 exhibited lower energy scores for caspase-3, cytochrome C, P53 and Bax than reference drugs[33] . Active caspase 3 degrades various intracellular proteins, leading to controlled cell dismantling. Caspase-3 had a high affinity for compound 7 (-10.09 Kcal/mol) compared to the Pac-1 standard anticancerous drug (-9.35 Kcal/mol). Cytochrome C is a critical mediator and biomarker of mitochondria-mediated apoptosis. Cytochrome C showed a binding score (-12.73 kcal/mol) to compound 7 while the anticancerous drug methazolamide showed a binding score (-10.34 kcal/mol). *p53* gene is the most commonly mutated gene in a wide range of human cancers, with mutations estimated to occur in approximately 50% of all cancer cases. The widespread occurrence of *p53* mutations across different cancer types highlights its critical role in tumor development and potential for targeting *p53* pathways in cancer treatment strategies[34]. The free binding energy score of P53 to compound 7 was (-9.79 kcal/mol) lower than that of Pifithrin b (-7.86 kcal/mol). As many chemotherapeutic agents have been proven to induce apoptosis in cancer cells, it has been proposed that targeting the regulators of apoptosis could be a promising approach for discovering new anticancer drugs.

Conclusion

In conclusion, compound 7 is an original molecule that was synthesized for the first time in this study. The side effects of standard treatments have motivated the development of new drugs. *In vitro* experiments have shown that compound 7 has a toxic effect on cancer cells but has no impact on control cells, highlighting its significance in this context. In addition, it induces apoptosis. Molecular docking studies revealed that the compound interacts with important protein targets, such as caspase-3, P53, cytochrome c, and Bax. The ADME analysis indicated that the molecule could potentially be developed into a drug. These findings indicate that the molecule possesses considerable potential as a therapeutic agent.

Finding statement

This study was funded by the Scientific Research Projects Coordination Unit of the Istanbul University. Project number: 36733. The Scientific Research Projects Coordination Unit of the Istanbul, UniversityCerrahpasa partially supported this study. Project number: 36176.

Author contribution statement

EHA, BG performed cell viability and caspase-3/7 assay, FO, KA, FV and NO performed chemical synthesis of anthraquinone derivates, HÇ contributed to flow analyses, MŞ performed molecular docking and ADME studies, BG, EHA designed the experiments and wrote the paper.

Conflict of interests

The authors declare that there are no conflict of interest.

References

1 Libson S, Lippman M (2014) A review of clinical aspects of breast cancer. *Int Rev Psychiatry* 26:4-15. https://doi.org/10.3109/09540261.2013.852971

2 Anand U, Dey A, Chandel AKS, Sanyal R, Mishra A, Pandey DK, De Falco V, Upadhyay A, Kandimalla R, Chaudhary A, Dhanjal JK, Dewanjee S, Vallamkondu J, Perez de la Lastra JM (2023) Cancer chemotherapy and beyond: Current status, drug candidates, associated risks and progress in targeted therapeutics. *Genes Dis* 10:1367-1401. https://doi.org/10.1016/j.gendis.2022.02.007

3 Oliveira LA, Nicolella HD, Furtado RA, Lima NM, Tavares DC, Corrêa TA, Almeida MV (2020) Design, synthesis, and antitumor evaluation of novel anthraquinone derivatives. *Medicinal Chemistry Research* 29:1611-1620. https://doi.org/10.1007/s00044-020-02587-4

4 Cheng, G., Liu, Z., Zheng, Z., Song, F., Zhuang, X., & Liu, S. (2022). Cell metabolomics reveals the potential mechanism of aloe emodin and emodin inhibiting breast cancer metastasis. *International Journal of Molecular Sciences*, *23*(22), 13738.

5 Sougiannis AT, Enos RT, VanderVeen BN, Velazquez KT, Kelly B, McDonald S, Cotham W, Chatzistamou I, Nagarkatti M, Fan D, Murphy EA (2021) Safety of natural anthraquinone emodin: an assessment in mice. *BMC Pharmacol Toxicol* 22:9. https://doi.org/10.1186/s40360-021-00474-1

6 Staffieri S, Russo V, Oliva MA, Alborghetti M, Russo M, Arcella A (2023) Aloe-Emodin Overcomes Anti-Cancer Drug Resistance to Temozolomide and Prevents Colony Formation and Migration in Primary Human Glioblastoma Cell Lines NULU and ZAR. *Molecules* 28. https://doi.org/10.3390/molecules28166024

7 Du Y, Zhang J, Tao Z, Wang C, Yan S, Zhang X, Huang M (2019) Aloe emodin exerts potent anticancer effects in MIAPaCa-2 and PANC-1 human pancreatic adenocarcinoma cell lines through activation of both apoptotic and autophagic pathways, sub-G1 cell cycle arrest and disruption of mitochondrial membrane potential (LambdaPsim). *J BUON* 24:746-753

8 Yang L, Li J, Xu L, Lin S, Xiang Y, Dai X, Liang G, Huang X, Zhu J, Zhao C (2019) Rhein shows potent efficacy against non-small-cell lung cancer through inhibiting the STAT3 pathway. *Cancer Management and Research*:1167-1176

9 Zhang H, Ma L, Kim E, Yi J, Huang H, Kim H, Raza MA, Park S, Jang S, Kim K, Kim SH, Lee Y, Kim E, Ryoo ZY, Kim MO (2023) Rhein Induces Oral Cancer Cell Apoptosis and ROS via Suppresse AKT/mTOR Signaling Pathway In Vitro and In Vivo. *Int J Mol Sci* 24. https://doi.org/10.3390/ijms24108507

10 Tian W, Li J, Su Z, Lan F, Li Z, Liang D, Wang C, Li D, Hou H (2019) Novel Anthraquinone Compounds Induce Cancer Cell Death through Paraptosis. *ACS Med Chem Lett* 10:732-736. https://doi.org/10.1021/acsmedchemlett.8b00624

11 Tikhomirov AS, Tsvetkov VB, Volodina YL, Litvinova VA, Andreeva DV, Dezhenkova LG, Kaluzhny DN, Treshalin ID, Shtil AA, Shchekotikhin AE (2022) Heterocyclic ring expansion yields anthraquinone derivatives potent against multidrug resistant tumor cells. *Bioorg Chem* 127:105925. https://doi.org/10.1016/j.bioorg.2022.105925

12 Su Z, Li Z, Wang C, Tian W, Lan F, Liang D, Li J, Li D, Hou H (2019) A novel Rhein derivative: Activation of Rac1/NADPH pathway enhances sensitivity of nasopharyngeal carcinoma cells to radiotherapy. *Cell Signal* 54:35-45. https://doi.org/10.1016/j.cellsig.2018.11.015

13 Kang J, Zhong Y, Tian W, Li J, Li X, Zhai L, Hou H, Li D (2021) A novel anthraquinone-quinazoline hybrid 7B blocks breast cancer metastasis and EMT via targeting EGFR and Rac1. *Int J Oncol* 58. https://doi.org/10.3892/ijo.2021.5199

14 Martins-Teixeira MB, Carvalho I (2020) Antitumour Anthracyclines: Progress and Perspectives. *ChemMedChem* 15:933-948. https://doi.org/10.1002/cmdc.202000131

15 Yeap S, Akhtar MN, Lim KL, Abu N, Ho WY, Zareen S, Roohani K, Ky H, Tan SW, Lajis N, Alitheen NB (2015) Synthesis of an anthraquinone derivative (DHAQC) and its effect on induction of G2/M arrest and apoptosis in breast cancer MCF-7 cell line. *Drug Des Devel Ther* 9:983-992. https://doi.org/10.2147/DDDT.S65468

16 Qun, T., Zhou, T., Hao, J., Wang, C., Zhang, K., Xu, J., ... & Zhou, W. (2023). Antibacterial activities of anthraquinones: structure–activity relationships and action mechanisms. *RSC Medicinal Chemistry*, *14*(8), 1446-1471.

17 Ozkok, F., Sezgın Mansuroglu, D., Öz, P., Asgarova, K., Şahin, Y. M., Onul, N., Çatal, T.(2024). Synthesis of a novel thio-anthraquinone derivative-based tissue dye. *Revue Roumaine De Chimie* , 69(5-6), 301-302.

18 Celik, S., Vagifli, F., Akyuz, S., Ozkok, F., Ozel, A. E., Dosler, S., Onul, N.(2022). Synthesis, vibrational spectroscopic investigation, molecular docking, antibacterial and antimicrobial studies of a new anthraquinone derivative compound. *Spectroscopy Letters* , (55), 259-277.

19 Ozkok, F.; Sahin, Y. M. Biyoaktif Antrakinon Anologlarının Sentezine Yonelik Ozgun Metot Gelistirilmesi, TURKIYE, Patent, TR 2016/19610.

20 Freshney RI (2005) Basic Principles of Cell Culture. In: *Culture of Cells for Tissue Engineering*. pp 1-22. https://doi.org/https://doi.org/10.1002/0471741817.ch1

21 Kumar, P., Nagarajan, A., & Uchil, P. D. (2018). Analysis of cell viability by the MTT assay. *Cold spring harbor protocols*, *2018*(6), pdb-prot095505.

22 Kumar R, Saneja A, Panda AK (2021) An Annexin V-FITC-Propidium Iodide-Based Method for Detecting Apoptosis in a Non-Small Cell Lung Cancer Cell Line. *Methods Mol Biol* 2279:213-223. https://doi.org/10.1007/978-1-0716-1278-1_17

23 Daina A, Michielin O, Zoete V (2017) SwissADME: a free web tool to evaluate pharmacokinetics, drug-likeness and medicinal chemistry friendliness of small molecules. *Sci Rep* 7:42717. https://doi.org/10.1038/srep42717

24 Di Muzio, E., Toti, D., & Polticelli, F. (2017). DockingApp: a user friendly interface for facilitated docking simulations with AutoDock Vina. *Journal of Computer-Aided Molecular Design*, *31*, 213-218.

25 Fuente-Garcia C, Sentandreu E, Aldai N, Sentandreu MA (2022) Optimization of a fluorogenic assay to determine caspase 3/7 activity in meat extracts. Food Sci Technol Int 28:128-134. https://doi.org/10.1177/1082013221993577

26 Malik, M. S., Alsantali, R. I., Jassas, R. S., Alsimaree, A. A., Syed, R., Alsharif, M. A., ... & Ahmed, S. A. (2021). Journey of anthraquinones as anticancer agents–a systematic review of recent literature. *RSC Advances*, *11*(57), 35806-35827.

27 Carvalho C, Santos RX, Cardoso S, Correia S, Oliveira PJ, Santos MS, Moreira PI (2009) Doxorubicin: the good, the bad and the ugly effect. *Curr Med Chem* 16:3267-3285. https://doi.org/10.2174/092986709788803312

28 Siddamurthi, S., Gutti, G., Jana, S., Kumar, A., & Singh, S. K. (2020). Anthraquinone: a promising scaffold for the discovery and development of therapeutic agents in cancer therapy. *Future medicinal chemistry*, *12*(11), 1037-1069.

29 Scabini M, Stellari F, Cappella P, Rizzitano S, Texido G, Pesenti E (2011) In vivo imaging of early stage apoptosis by measuring real-time caspase-3/7 activation. *Apoptosis* 16:198-207. https://doi.org/10.1007/s10495-010-0553-1

30 Wu S, Zhou X, Li F, Sun W, Zheng Q, Liang D (2024) Novel Anthraquinone-Based Benzenesulfonamide Derivatives and Their Analogues as Potent Human Carbonic Anhydrase Inhibitors with Antitumor Activity: Synthesis, Biological Evaluation, and In Silico Analysis. *International Journal of Molecular Sciences* 25:3348

31 Malladi SM, Sadhu SP, Pandey DK, Yarla NS (2023) Molecular docking studies and In-silico ADMET profile analysis of Triphala plant constituents morin and 9, 10-anthraquinone as potential inhibitors of human estrogen receptor alpha. *Research Journal of Pharmacy and Technology* 16:3759-3766

32 Ahmad W, Ansari MA, Alsayari A, Almaghaslah D, Wahab S, Alomary MN, Jamal QMS, Khan FA, Ali A, Alam P, Elderdery AY (2022) In Vitro, Molecular Docking and In Silico ADME/Tox Studies of Emodin and Chrysophanol against Human Colorectal and Cervical Carcinoma. Pharmaceuticals (Basel) 15. https://doi.org/10.3390/ph15111348

33 Hussain SP, Harris CC (2000) Molecular epidemiology and carcinogenesis: endogenous and exogenous carcinogens. *Mutat Res* 462:311-322. https://doi.org/10.1016/s1383-5742(00)00015-6

34 Marei HE, Althani A, Afifi N, Hasan A, Caceci T, Pozzoli G, Morrione A, Giordano A, Cenciarelli C (2021) p53 signaling in cancer progression and therapy. *Cancer Cell Int* 21:703. https://doi.org/10.1186/s12935-021-02396-8